

Examples of the Influence of Residual stresses on Fracture

W. Cheng¹ and I. Finnie²

Abstract Generally compressive residual stresses increase the resistance of a part to fracture while tensile residual stress degrades strength. It will be shown that the local compressive residual stresses and the subsurface cracks produced by scribing, at very low loads, are responsible for the low tensile strength of glass specimens. Also, if metal parts containing surface cracks are subjected to pressure such as shot-peening, which produces high near surface residual compressive stresses, the initial end of the crack will experience tensile loading. This paper explains these phenomena using procedures based on LEFM. A method for residual stress measurement using LEFM solutions is also reviewed.

1. BEAR, Inc.
Berkeley, CA 94710
e-mail: weilicheng@home.com

2. James Fife, Professor Emeritus
Dept. of Mech. Eng., University of California
Berkeley, CA 94720
e-mail: finnie@me.berkeley.edu

Introduction

The literature on cracking due to a sliding indenter, a process often referred to as scribing or scratching, goes back 80 years ago, when Griffith's classic work appeared. The scribing process will be described, and it is seen that "median" cracks propagate downwards, below the indenter, in glass at loads as low as 0.014 N. The present work is based on loading a sub-surface crack and analyzes the effect of loading rate in a moist environment in a different manner from previous work by others. The present work estimates the strength of glass in the presence of subsurface flaws produced by scratching. An upper bound is observed by considering an inert environment. A lower bound is obtained for the strength of glass in moist air.

A related problem is the residual stresses induced by shot-peening or laser surface treatment. These are shown to have a profound effect on surface flaw detection. It is also shown that the solutions for LEFM leads to a new method for residual stress measurement.

The Strength of Glass Following Scribing

The scribing process shown in Fig. 1 introduces a zone of deformation under the indenter which we describe as "the plastic zone" due to a combination of compression and shear. The first crack to form, described as the median crack, propagates from the base of the plastic zone as shown in Fig. 2. Currently, the concept that surface flaws are inherent in glass is a common concept. For example, in the well known book by McClintock and Argon (1966) it is stated that "In some brittle solid, such as inorganic glass, cracks are formed only at the free surfaces". To study this assumption, we take a simple model in which the inherent flaw is treated as an edge crack and residual stresses are ignored. Taking a fracture toughness K_{IC} of $0.76 \text{ MN/m}^{3/2}$ and fracture stress of soda lime glass in a moist environment of 70 MPa leads to an estimate of crack size of $a = [K_{IC}/(1.12 \sigma)]^2 / \pi = 30 \mu\text{m}$. Immediately, we can draw two contradictory conclusions, first, such a flaw size should be detectable by optical or scanning electron microscope (SEM). Second, to our knowledge no such surface cracks have been observed directly. It is tempting by saying that the crack faces are touching. However, SEM examination of glass subjected to bending loads, which should separate the faces of a closed crack, has not revealed cracks. This suggests that strength impairing flaws are so close to the surface that they may be removed by surface melting or etching.

The most likely source of the damage described is scratching or scribing by small abrasive particles. As shown in Fig. 2 a median crack initiates at the base of the plastic zone. The lowest load we have observed for such median crack initiation is 0.014 N. Since the size of the median crack, as just over the threshold load, is only several micrometers, its influence on the fracture stress would be expected to be small if residual stresses are absent. However, scribing produces a high compressive stress in the plastic zone which prevents subsurface flaws from growing into the plastic zone. Also, the plastic zone exerts an opening force at the lower crack tip shown in Fig. 2. The fact that the median crack is often observed to grow after scribing shows the significance of the residual stress. In recent work, we have obtained the residual stress distribution below the plastic zone and have obtained the stress intensity factor for a subsurface flaw (Cheng and Finnie 1992) as shown in Fig. 3, the estimated fracture stress of soda lime glass is greatly reduced by the presence of the compressive residual stress near the surface. The prediction for moist and inert environments agrees well with the reported strength values in literature.

Surface and Near Surface Residual Stresses and Their Influence on Flaw Detection

We now consider the case of a flaw which exists before near surface residual stresses are introduced by shot peening. A typical distribution of residual stresses is shown schematically in Fig. 4. The high compressive stresses near the surface greatly increase the resistance of a part to crack initiation. However, if a surface flaw is already present, the compressive stress near the surface effectively closes the mouth of the crack and may prevent its detection by dye penetrants. If the crack size is larger than the depth to which compressive stress is present, the crack tip will be subjected to tensile stresses. The displacement caused by releasing the compressive stress on the surface must be computed to estimate the force required to open the crack so that it can be detected.

To obtain the displacement/rotation due to a point load/moment for a cracked body, we use Castigliano's theorem (Tada et al. 1973). For two dimensional part of unit dimension normal to the x-y plane subjected to Mode I loading, the displacements v on the surface at a distance s from the crack plane may be obtained by introducing the virtual forces F , shown in Fig. 6. This leads to

$$v(a,s) = \frac{\partial U}{\partial F} = \frac{1}{E} \int_0^a K_I(a) \frac{\partial K_I^f(a,s)}{\partial F} da \quad (1)$$

where a is the crack length, $E' = E$ and $E/(1-\mu^2)$ for plane stress and plane strain respectively, U is the change of the strain energy due to the crack, K_I and K_I^f are the stress intensity factors for an arbitrary stress on the crack faces and the virtual force F respectively. Only the opening at the mouth of the crack is of interest (twice of v under load F) so $s = 0$. For simplicity, the residual stress due to shot peening is approximated by a uniform stress σ_r from $a = 0$ to b as shown in Fig. 3. The corresponding K_I is negative and hence fictitious but is needed to obtain the displacements required for subsequent calculation. Using the expressions for K_I and K_I^f given by Cheng and Finnie (1988) and Tada et al. (1973), Eq. (1) becomes

$$v_r(a) = 2.9 \frac{F_r}{E} a H\left(\frac{b}{a}\right) \quad \text{with} \quad H\left(\frac{b}{a}\right) = \frac{b}{a} \int_{b/a}^1 f(z) dz \quad a \leq b \quad (2)$$

where

$$f(z) = 1 + \left(\frac{2}{B}\right) \left(1 + \frac{3}{28} \frac{b/a}{z}\right) \cos^2 \left(\frac{b/a}{z}\right) \quad (3)$$

In Eq. (3) the dummy variable z represents the ratio of any intermediate crack size to the final crack size. Displacement v_r would only appear when the crack is entirely opened by external loading. To open the crack, we apply a uniform tensile stress σ_0 over crack faces and the resulting displacement v_0 can be obtained by setting $b/a = 1$ in Eq. (3). Thus, the stress required for opening the crack is obtained by equating v_0 and v_r . This leads to $\sigma_0 = \sigma_r H(b/a)$. Figure 5 shows the ratio of σ_0/σ_r against b/a . It is seen that the opening stress required decreases as the size of the crack increases. Now it is possible to determine the tensile stress required to open the crack for detection.

The Crack Compliance Method for Through-the-Thickness Residual Stress Measurement

The inverse problem of determining residual stresses from measurements of strain, displacement or stress intensity factor as a crack is introduced into a part received little attention until the past decade. Vaidyanathan and Finnie [1971] showed that measurements of stress intensity factor as a function of crack length could be used to deduce the residual stress due to a butt-weld between two plates. However, the experimental technique using a photoelastic coating to measure the stress intensity factor, was time consuming and unsuited to general application. A more useful procedure, which was subsequently extended to a variety of configurations, was developed by Cheng and Finnie [1985]. This involved measurements of strain as a function of crack depth to deduce the axial residual stress in a circumferentially welded cylinder. We refer to this approach as the "crack compliance method" because it is closely related to the solutions for the compliance due to a crack. Similar procedures were presented later by Fett [1987], Ritchie and Leggett [1987] and Kang, et al [1989].

To explain the basis of the method we consider the strip shown in Fig. 6 which contains residual stresses $\sigma_y(x)$. For near surface stress measurement, which will be discussed later, one or more strain gages are located close to the mouth of the crack. For through-the-thickness stress measurement a strain gage is located on the back face of the strip. In either case the normal strain $\epsilon(a,y)$ at location $y = s$ produced by introducing a crack of depth a is given by differentiating Eq. (2),

$$\epsilon(a,s) = \frac{Mv(a,s)}{Ms} = \frac{M^2 U}{MFM_s} = \frac{1}{E} \int_0^a K_I(a) \frac{M^2 K_I^f(a,s)}{MFM_s} da \quad (4)$$

Since strains can be measured very precisely with strain gages, Eq. (4) provides a more useful approach than displacement or stress intensity factor measurement.

Consider a body with a residual stress distribution expressed in terms of a series expansion of order n with amplitude factor A_i defined for the i^{th} order term. We now introduce a crack or a very thin cut of progressively increasing depth to the body while measuring the change of the strain at location s as shown in Fig. 6. From linear superposition K_I can be expressed as

$$K_I = \sum_{i=0}^n A_i K_I^i(a) \quad (5)$$

where K_I^i is the stress intensity factor corresponding to the stress given by the i^{th} term in the series expansion. Equation (5), when combined with Eq. (4), leads to

$$\epsilon_j = \sum_{i=0}^n A_i C_i(a_j, s) \quad \text{with} \quad C_i(a_j, s) = \frac{1}{E} \int_0^{a_j} K_I^i(a) \frac{M^2 K_I^f(a,s)}{MFM_s} da \quad (6)$$

where ϵ_j is the strain measured when crack depth equals a_j and C_i is crack compliance functions. When the number of the strain measurements is greater than $n+1$, the unknown A_i can be determined

using a least squares fit which reduces the average error over all data points to the minimum.

Crack compliance functions for through-thickness residual stress measurements have been obtained for a number of geometries. Figure 7 shows a residual hoop stress distribution measured in a water-quenched thick-walled ring. The agreement with numerical computation and X-ray measurement at the surface is very good. The method is especially useful when the stress to be measured varies rapidly both with the distance from the plane of the cut and with the depth of cutting. Such a situation arises for example at the toe of a fillet weld or at any other welded junction. X-ray and layer removal techniques are not well suited to such problems.

The Slit Compliance Method for Near-Surface Residual Stresses Measurement

In this case the width of the cut is usually not negligible, and the compliance functions for a slit instead of a crack are obtained using the body force method [Nisitani, 1978]. Similar to the hole-drilling method, strain gages are located on the surface near the cut. However, the actual distance measured from the strain gage to the cut is used in the computation of the compliance functions to eliminate the mis-alignment error which is often associated with the hole-drilling method. The strain response obtained by the slit compliance method has been shown to be more than twice of that obtained by the hole-drilling [Cheng and Finnie, 1993].

Residual stresses produced by surface treatment or cladding usually vary rapidly over a small distance below the surface. A least squares fit using a single continuous function may become unstable for numerical computation as the order of prediction increases. To solve this problem, we have developed a general procedure combining the least squares fit with lower order overlapping piecewise functions [Gremaud, et al. 1994] and implemented it for estimation of near surface stresses. Experimental results show that this procedure is capable of measuring stresses with a very steep gradient which failed to be detected by the X-ray diffraction method. Figure 8 shows a comparison of the residual stress distribution in a laser-treated specimen measured by the slit compliance and by the X-ray method with layer removal. The slit compliance method has also been used to measure the stress due to shot-peening and shows good agreement with X-ray measurements.

Using a specially made electrode for EDM, cuts of almost uniform depth can be introduced on a curved surface. Measurements can now be made at locations such as inside a valve body where other techniques would be impossible to implement without cutting the specimen apart.

Discussion

Griffith's classic work is revisited to show the influence of residual stresses on the tensile strength of glass in moist and inert environments.

The phenomenon of crack closure due to the residual stress in the wake of a propagating crack is familiar to those working in fatigue. However, the fact that surface compressive stresses may lead to closing of the crack mouth does not appear to have been fully appreciated in the area of non-destructive inspection for cracks.

The equivalence of energy release rate and the stress intensity factor, which is required to derive Eqs. (2) and (6), was shown in Irwin's classic paper in 1957. However, apart from a limited step in 1971, the use of LEFM for residual stress measurement has been developed only in the past decade. We have reviewed this recent work which appears to improve measurement procedures for many practical configurations.

References

- Cheng, W. and Finnie, I., 1985, "A Method for Measurement of Axisymmetric Residual Stresses in Circumferentially Welded Thin-Walled Cylinders," ASME, J. of Eng. Mat. and Tech., **106**, 181-185.
 Cheng, W. and Finnie, I., 1988, " K_I Solution for an Edge-Cracked Strip," Eng. Fracture Mech., **31**, 201-207.

- Cheng, W. and Finnie, I., 1992, "A Prediction on the Strength of Glass Following the Formation of Subsurface Flaws by Scribing," J. of the American Ceramic Society, **75**, 2565-2572.
- Cheng, W. and Finnie, I., 1993, "A Comparison of the Strains due to Edge Cracks and Cuts of Finite Width With Applications to Residual Stress Measurement", ASME J. of Eng. Mat. and Tech., **115**, 220-226.
- Fett, T., 1987, "Bestimmung von Eigenspannungen mittels bruchmechanischer Beziehungen," VDI-Verlag GmbH, Düsseldorf , 92-94.
- Gremaud, M., Cheng, W., Prime, M. B. and Finnie, I., 1994, "The Compliance Method for Measurement of Near Surface Residual Stresses - Analytical Background," ASME J. of Eng. Mat. and Tech. **116**, 550-555.
- Griffith, A. A., 1921, "The Phenomena of Rupture and Flow in Solids," Phil Trans., **221A**, 163-198.
- Kang, K. J., Song, J. H. and Earmme, Y. Y., 1989, "A Method for the Measurement of Residual Stresses Using a Fracture Mechanics Approach," J. of Strain Analysis, **24**, 23-30.
- McClintock, F. A. and Argon, A. S., 1966, Mechanical Behavior of Materials, P. 496. Addison-Wesley, Reading, MA.
- Nisitani, H., 1987, Stress Analysis of Notch Problems, Mechanics of Fracture Vol. 5, Edited by G. C. Sih, Noordhoff Int. Publishing.
- Ritchie, D. and Leggatt, R. H., 1987, "The Measurement of the Distribution of Residual Stresses Through the Thickness of a Welded Joint," Strain, 61-70.
- Tada, H., Paris, P. and Irwin, G., 1973, The Stress Analysis of Cracks Handbook, Del Research Corporation, PA.
- Vaidyanathan, S. and Finnie, I., 1971, "Determination of Residual Stresses from Stress Intensity Factor Measurement," Trans ASME, J. Basic Eng. **93D**, 242-246.

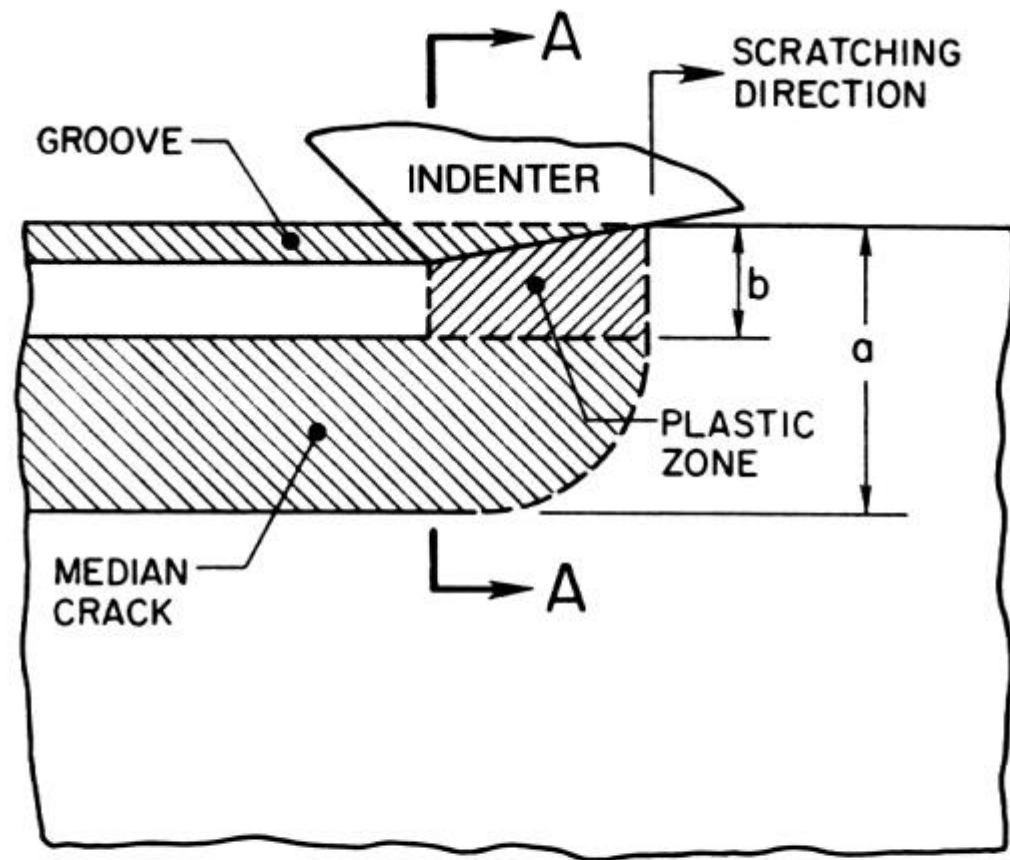


Fig. 1. Schematic cross section of scratching viewed perpendicular to scratching direction.

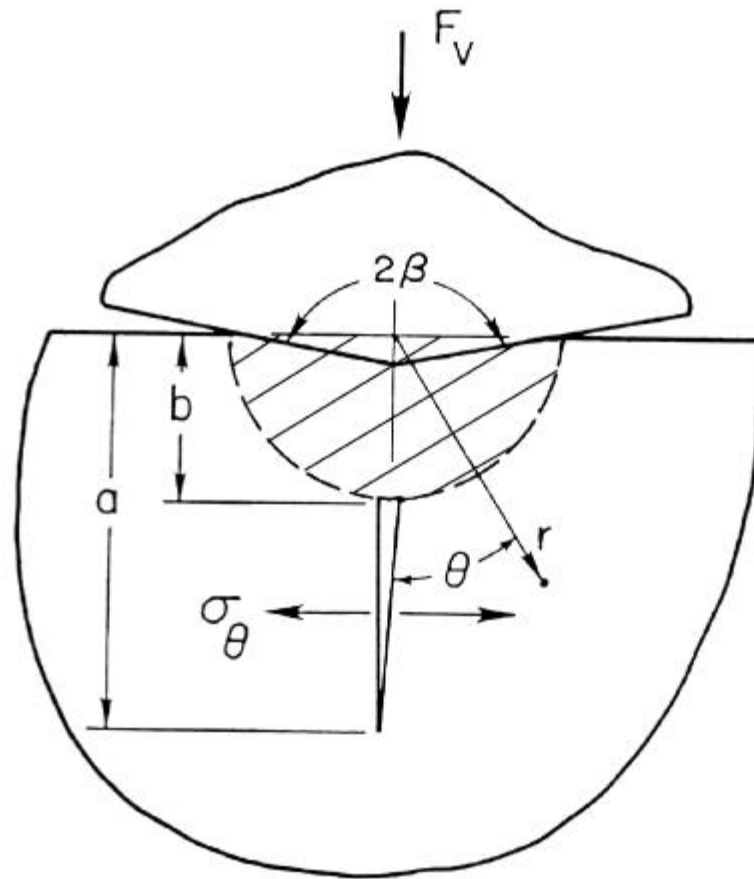


Fig. 2. Schematic view of the permanent deformation and a median crack looking in the direction AA shown in Fig. 1.

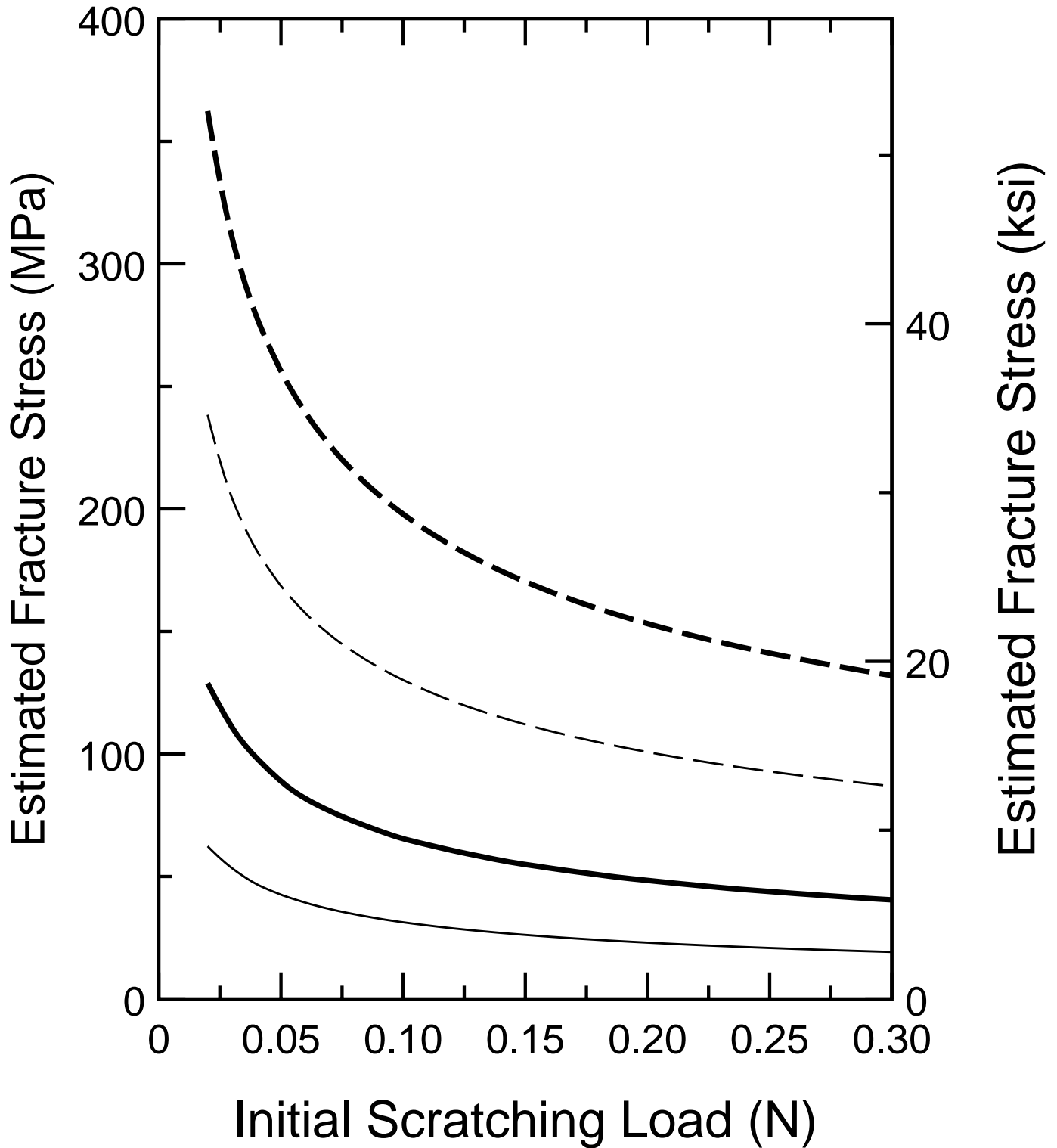


Fig. 3 Prediction of tensile strength of soda-lime glass as a function of scratching load dry air ignoring residual stress (heavy dashed line) and with residual stress (heavy solid line). For moist air the corresponding predictions are shown by the thin dashed and solid lines.

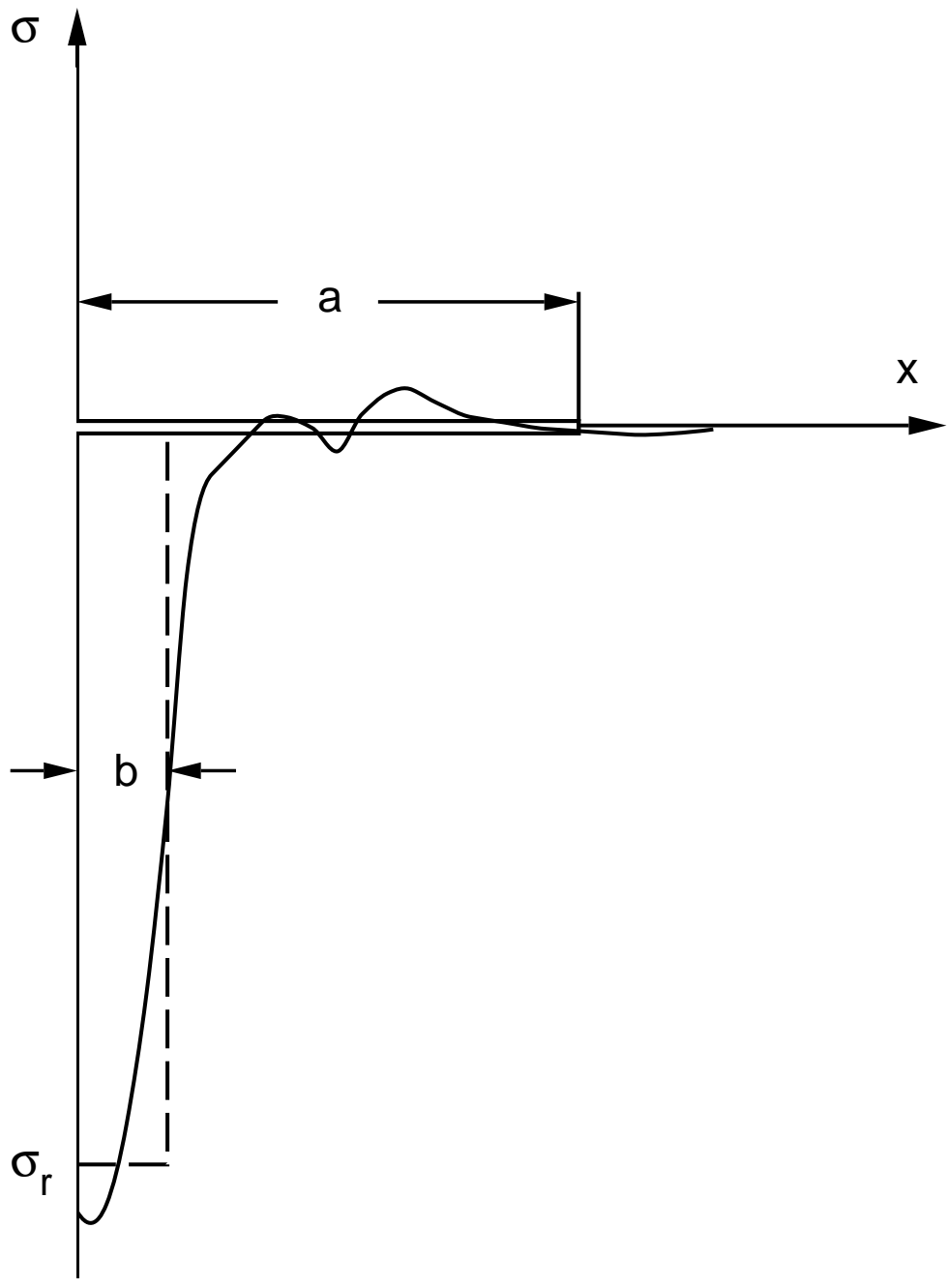


Fig. 4 Schematic of residual stress measured for a typical shot-peening application (solid line) and approximation by a rectangular distribution

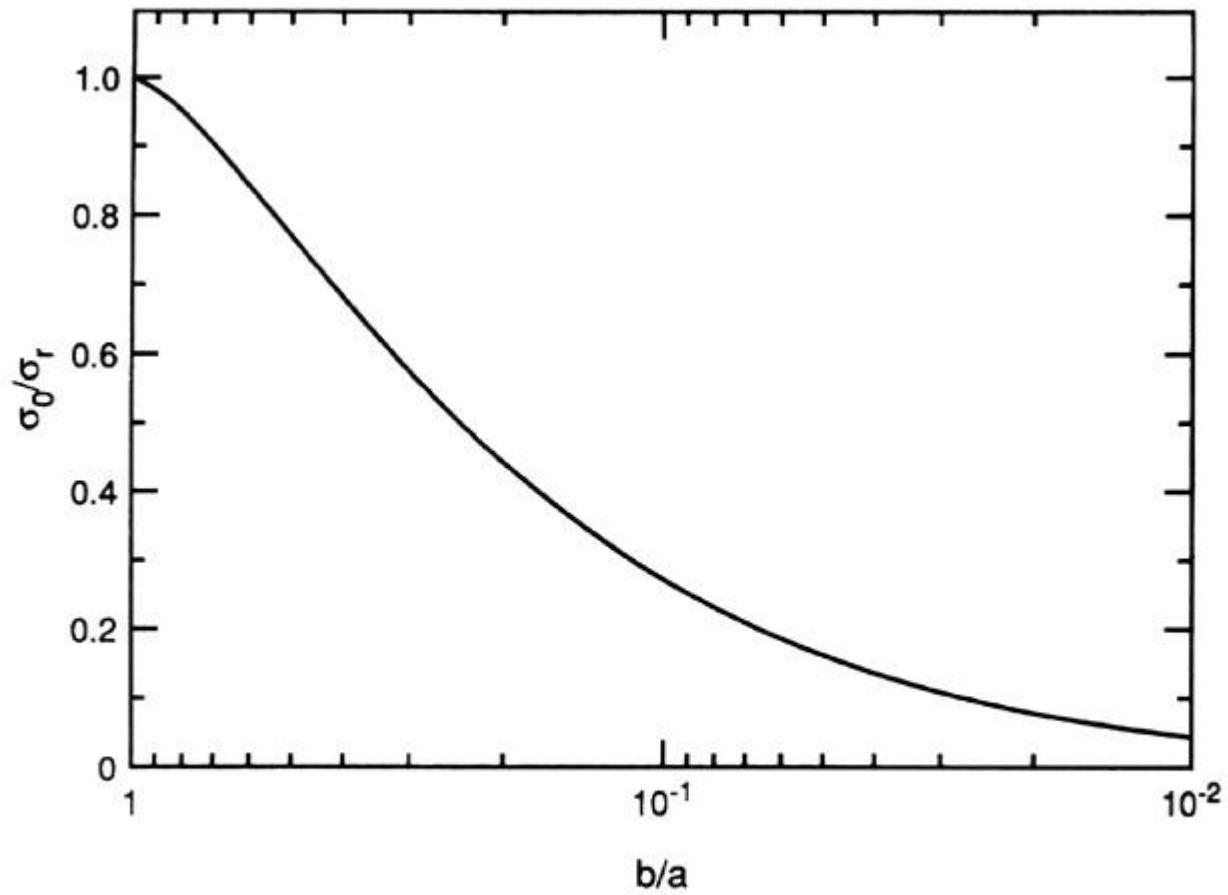


Fig. 5 The ratio of the opening stress to the magnitude of the residual stress as a function of b/a

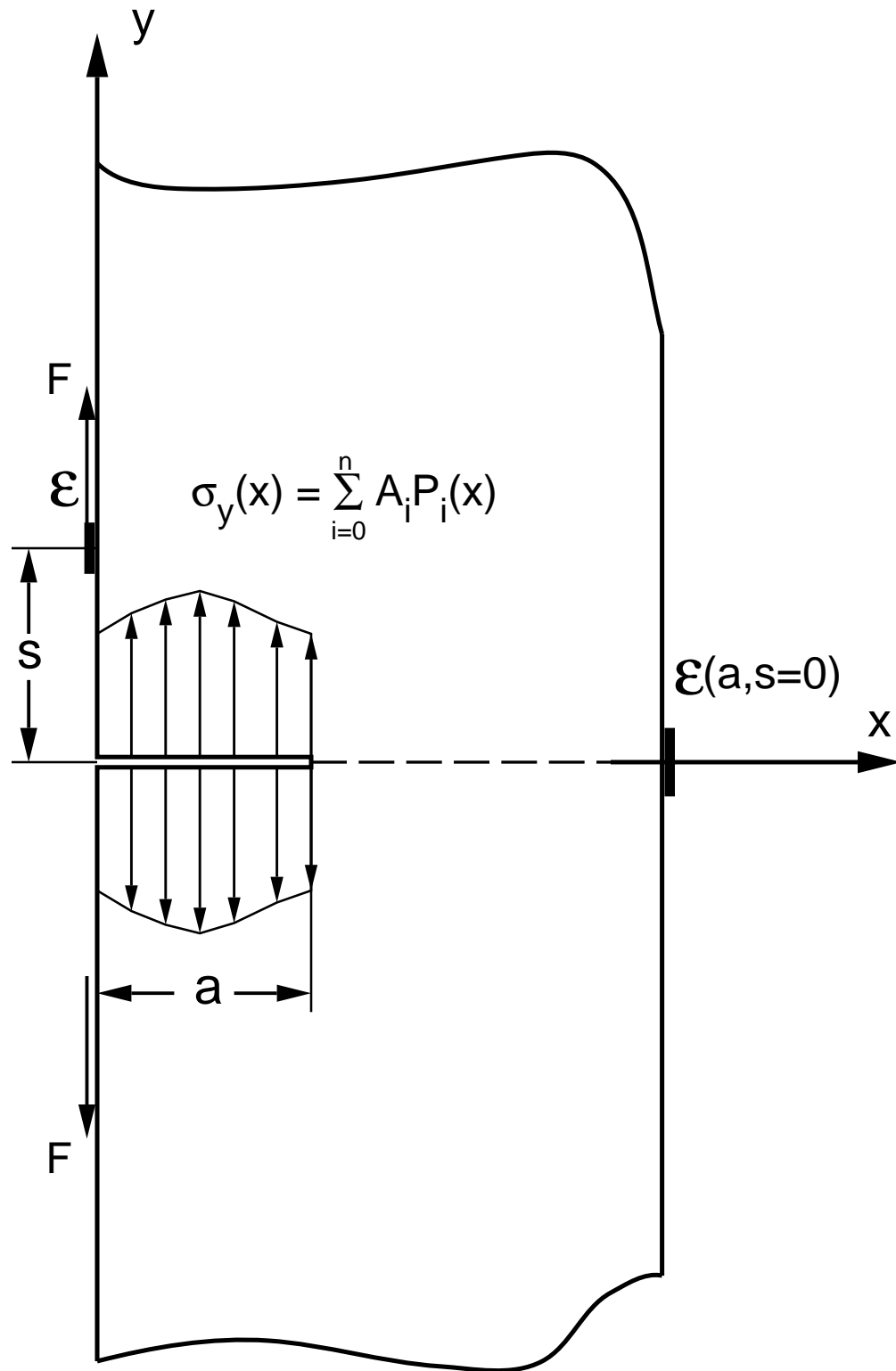


Fig. 6 A thin cut is introduced in a body with residual stress while strains are measured at selected locations

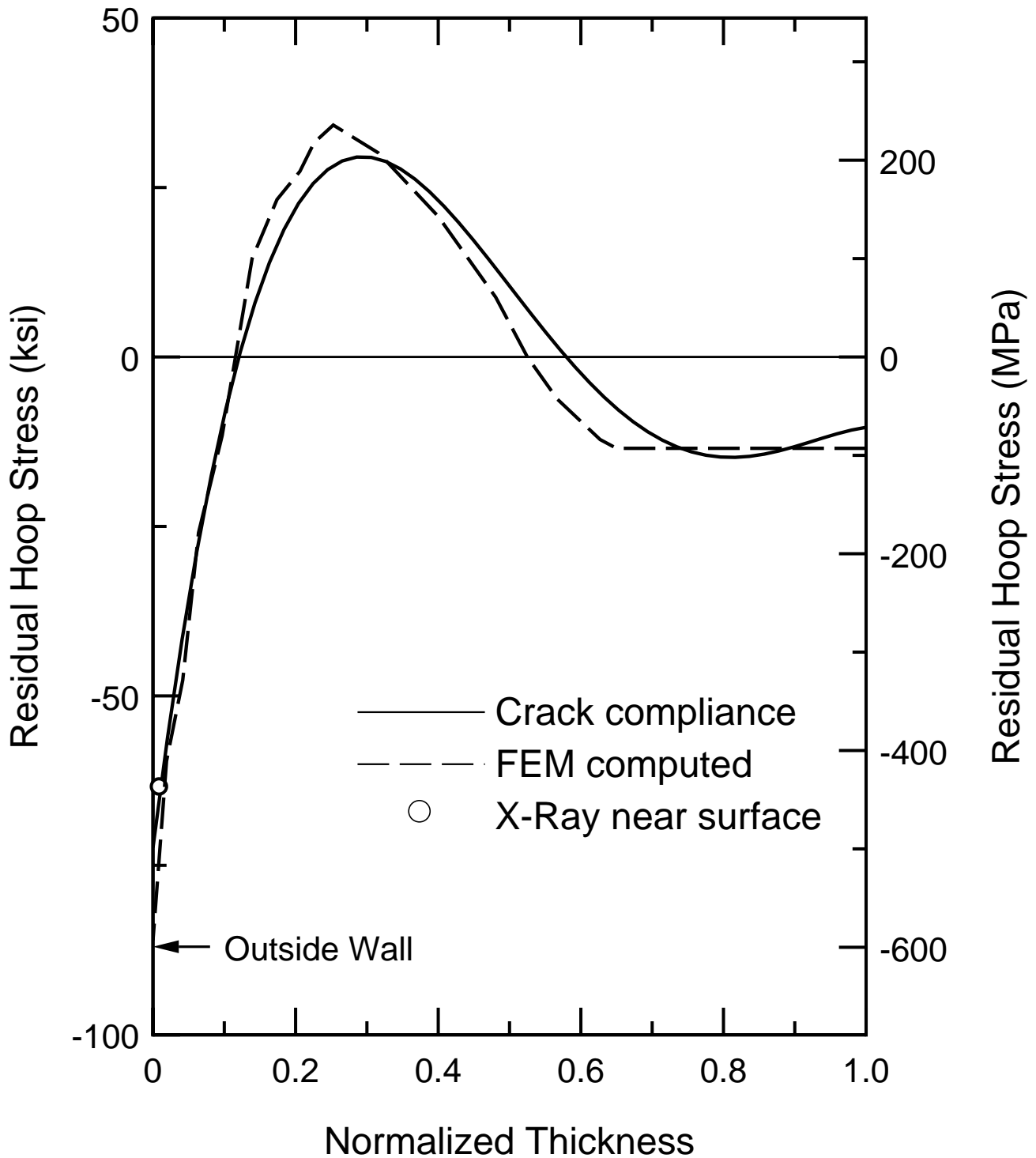


Fig. 7 Residual hoop stress in a water-quenched thick-walled ring measured by the present method (solid line) compared with numerical computation by FEM (dashed line). The near surface stress (data point) was measured by X-ray method.

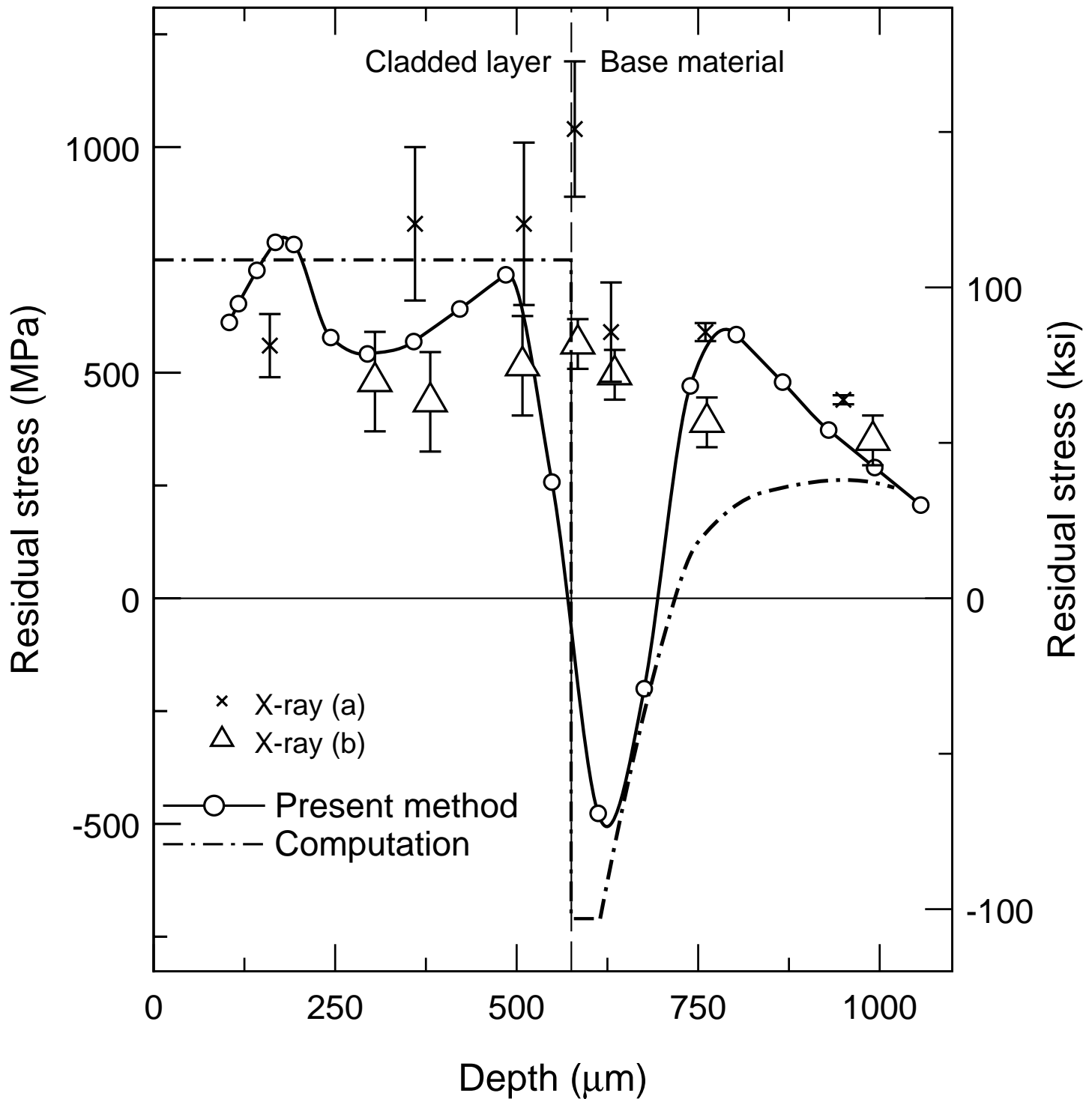


Fig. 8 Residual stress due to laser surface treatment measured by the present method and by the X-ray method from two independent laboratories. The dashed line represents approximate numerical computation